

Compact bulk-machined electromagnets for quantum gas experiments

K. Roux, B. Cilenti, V. Helson, H. Konishi, and J.P. Brantut^{1*†}

¹ Institute of Physics, École Polytechnique Fédérale de Lausanne, 1015 Lausanne, Switzerland

* jean-philippe.brantut@epfl.ch

† <http://lqg.epfl.ch>

June 7, 2021

Abstract

We present an electromagnet combining a large number of windings in a constrained volume with efficient cooling. It is based on bulk copper where a small pitch spiral is cut out and impregnated with epoxy, forming an ensemble which is then machined at will to maximize the use of the available volume. Water cooling is achieved in parallel by direct contact between coolant and the copper windings. A pair of such coils produces magnetic fields suitable for exploiting the broad Feshbach resonance of ^6Li at 832.2 G. It offers a compact and cost-effective solution for quantum gases experiments.

1 Introduction

Strong, homogeneous magnetic fields of the order of thousand Gauss are at the core of quantum gas experiments, from laser cooling and trapping [1] to the use of Feshbach resonances controlling the inter-atomic interactions [2]. As experimental apparatus become more and more complex, with more laser beams or high-aperture imaging systems to accommodate, space occupation as well as heat management constraints become more and more acute, calling for optimized and flexible electromagnet designs. Efforts in this direction have been reported in the past years, in particular novel designs for Zeeman slowers [3, 4], Bitter electromagnets [5–7] or improved heat management methods [8]. More compact systems of magnetic traps use in-vacuum electromagnets [9–11], or atom chips [12, 13], but those are not adapted to experiments requiring large homogeneous fields.

The common ground of these electromagnet concepts is the improvement over the widely used design based on wound copper wire (see for exemple [14]). This solution is privileged due to its robustness, and the use of hollow wire allows for water cooling with good contact between copper and the coolant. It suffers however from several drawbacks, the first being the need of parallel flow of coolant and electrical current, yielding a large coolant pressure drop across the magnet. Several parallel circuits of coolant fluid are then needed to limit temperature inhomogeneities in the coil. Another drawback is the lack of flexibility and poor

space occupation efficiency: hollow copper wires are restricted to several millimeters wide wires, restricting the number of windings in a given volume. In addition, the epoxy matrix and coolant circuit inlets and outlets restrict the fraction of volume actually used for current carrying copper.

The Bitter-type configuration addresses some of these drawbacks [5–7], in particular it offers very good heat management thanks to the parallel flow of coolant through the magnet, at the cost of requiring each winding to bear several coolant connections. Space occupation was addressed in a recent improvement where several layers are used to increase the number of windings [15]. Other alternatives include the use of mixed configurations where hollow copper is combined with bulk copper wires [16] in a single assembly, or a scheme with fully parallel cooling demonstrated in a few-windings coil directly machined from a bulk copper block [8].

In this article, we present electromagnets optimizing space occupation, offering very large shape flexibility while allowing to reach the high fields required for the use of Feshbach resonances in ${}^6\text{Li}$ [17]. Our design is based on a bulk copper plate in which a spiral is cut by wire erosion [8], and impregnated with epoxy. The resulting ensemble is machinable using standard tools, allowing for carving out ridges to maximize space occupation or holes for electrical connections and clamping. As a result, the limited volume of a reentrant vacuum viewport accommodates 31 windings over a single 22 mm thick layer. We present the detailed fabrication procedure of the ensemble, as well as performance in terms of magnetic fields and heat management, demonstrating the suitability of this approach for quantum gases experiments.

2 Concept and design

The maximum magnetic field that a coil electromagnet can produce is limited by the geometric constraints on the coil dimensions and the total allowable power dissipation. In designing electromagnets for cold atoms experiments, the dimensions are constrained by the vacuum systems and necessary optical access, which limits the distance to the atoms and restricts the total volume available for the current carrying coil. In addition, the electric current is limited by practical constraints such as the diameter of cables, heating at the contacts and availability of power supplies.

In our design, the electromagnet has to fit in the limited volume of a reentrant vacuum viewport, while allowing for the use of high-resolution optics. At the same time, a pair of such electromagnets shall achieve magnetic fields of hundreds of Gauss several centimeters below the coil, at the position of the atoms, in order to reach Feshbach resonances in ${}^6\text{Li}$ atoms, with a current limited to 440 A by the power supply. We meet these requirements using a coil comprising 31 turns horizontally stacked in a single 22 mm thick layer, depicted in figure 1, with a large aspect ratio of 23.9 for an individual winding.

With a fixed geometry, the performance is limited by power dissipation, which is achieved by forced convection with cold water. Two cooling regimes can be distinguished: cooling is either *flux-limited*, where the coolant and magnet are thermalized and heat removal is limited by the flow of water, or *transfer-limited* where heat transfer at the magnet-coolant interface is the limiting factor and the coolant temperature varies weakly across the system.

In our horizontal stack configuration, the electromagnet is cooled by cold water in direct contact with the upper surface of the coil allowing for very large fluxes at low pressure, as

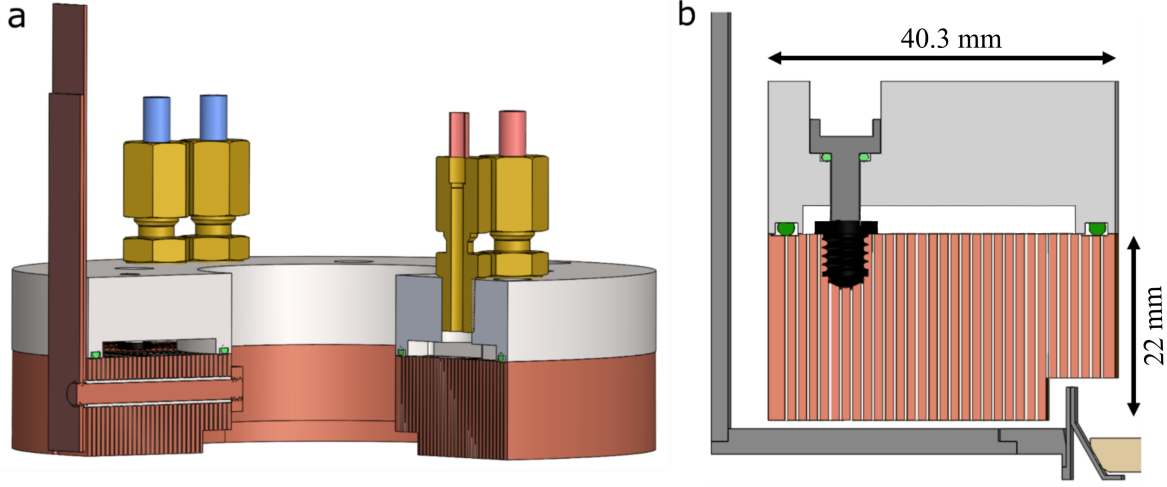


Figure 1: **a**: 3D Computer-assisted drawing of the electromagnet. The electromagnet comprises the coil with horizontally stacked windings, a cap creating a channel for water cooling, electrical and coolant connections. A ridge is machined in the coil to fit the geometry of the reentrant viewport, and a through hole allows for electrical current be carried from the inner to outer windings through the coil body. Electric current is injected and collected by a pair of flat cables running upward. **b**: Cut view of the electromagnet, showing blind threaded holes holding the cap and the coil together, in order to form a water-tight channel. The resulting assembly optimally fits the available space with current carrying copper.

described in figure 1, and we expect to operate in the *transfer-limited* regime. We first check that even for windings with a large aspect ratio, cooling on the upper surface is sufficient to ensure minimal temperature gradients across the coil. For a given current I in the windings, neglecting lateral heat flow between windings, the temperature difference between the top and bottom of the coil reads

$$\Delta T = \frac{I^2}{w^2} \frac{\rho_{\text{Cu}}}{2\lambda_{\text{Cu}}}, \quad (1)$$

with ρ_{Cu} and λ_{Cu} the electrical resistivity and heat conductivity of copper, respectively, and w the width of one winding. For a current of 400 A and $w = 1$ mm, we get $\Delta T = 3.4$ K, showing that gradients within the coil will be minimal.

The heat transfer at the copper-water interface depends on the nature of the flow. For a typical total flow rate in the coil of $0.23 \text{ l}\cdot\text{s}^{-1}$, a simple estimate based on the hydraulic diameter of the duct yields turbulent flow with a Reynolds number of $\sim 6.4 \cdot 10^3$ [18]¹. We deduce a heat transfer coefficient $h_w \sim 5 \cdot 10^3 \text{ W} \cdot \text{m}^{-2}\text{K}^{-1}$. In this configuration, convection is indeed the dominant heat transfer process, both within the fluid, where we estimate a Nusselt number of the order of 70, and between the coil and the coolant: to assess the relative roles of heat diffusion within the copper and heat exchange at the interface, we form the dimensionless ratio

$$\frac{h_w H}{2\lambda_{\text{Cu}}} = \frac{\Delta T}{\Delta T_w}, \quad (2)$$

¹The large aspect ratio and short length of the duct would call for a more detailed analysis of the flow, beyond the scope of the present work

with H the thickness of the coil, giving the ratio between the temperature differences across the copper coil ΔT and between the water and copper ΔT_w , which we expect to be ~ 0.2 . Interestingly, this does not depend on the interface area.

This shows that even with extreme aspect ratio for the coil windings, heat diffuses efficiently through the coil up to the water-copper interface, and that we operate in the transfer-limited regime in contrast to most designs [7, 14]. Operating in the transfer-limited regime has the advantage that heat removal is less sensitive to the water flux since the flux enters only through the heat transfer coefficient with a sub-linear dependence [18].

3 Manufacturing and assembly

Manufacturing of the electromagnet followed the concept of [8], where a coil is carved out from bulk copper rather than wound out of wires. As described below, a major advantage of this concept is that the thick body of the coils forms a single, rigid ensemble, which can then be shaped using standard lathe and milling machines. As long as machining does not significantly affect the windings, the final shape can fulfill a wide variety of space constraints, with negligible effects on the magnetic field distribution. We used this capability in order to carve out tapped holes for holding the cap, a through hole carrying current through the coil body from the inner to the outer part and an edge in order to fit the exact geometry of the reentrant viewport, as can be shown in figure 1.

3.1 Coil body

Manufacturing started from a 24 mm thick oxygen-free copper plate. Wire-erosion machining creates a spiral with a pitch of 1.3 mm, leaving a gap between consecutive windings of 0.38 mm. Fiber-glass reinforced plastic spacers were inserted between successive windings to preserve uniform spacing and ensure electrical insulation. After cleaning and drying, the spiral was impregnated with epoxy glue. We used commercial low viscosity, room-temperature curing epoxy², loaded with 10% of 0.25 μm fiber glass flake and 30% aluminium nitride (AlN) powder³. Preliminary tests showed that cracks can develop in the inter-windings regions due to thermal stress when using high temperature curing epoxy, hence the use of fiber glass load to reinforce the structure. We also found that the use of AlN load improves the heat dissipation from the inner and outer windings of the coils, which are not in direct contact with water.

The impregnated coil was then machined with a lathe in order to remove the excess glue and expose the copper on the coil facet to be water cooled. The resulting surface quality is high, as can be seen in figure 2. The assembly consists in more than 70% copper in volume. Blind threaded holes were machined on the top surface in order to hold the water cooling cap pressed against the coil, a transverse through-hole was drilled and an fiber-glass insulating tube glued inside to accommodate a 5.5 mm diameter copper screw carrying current from the inner to outer winding (see figure 1).

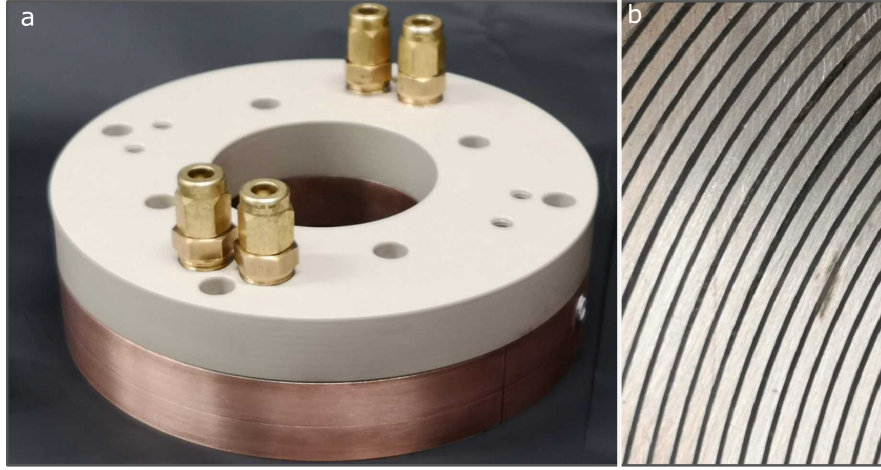


Figure 2: **a**: Photograph of the assembled electromagnet, showing the PEEK cap attached to the coil body, with coolant connections from the top. **b**: Close view of the top surface of the coil after glueing and machining, showing the successive windings separated by the electrically insulating epoxy. The width of a copper winding is 0.92 mm.

3.2 Electromagnet assembly

As shown in figure 1, the electromagnet mainly consists in the coil and the plastic cap creating the water cooling channel and holding the ensemble together. The cap is a U-shaped PEEK⁴ part forming a 3 mm high channel on the top surface of the coil, with a cross section area of 102 mm². To increase the water flux, the channel is split in two half-circles with separate inlets. The cap is attached to the coil body by 8 titanium screws directly fitting in threaded holes machined on the top surface of the coil. PEEK inserts fit into the holes to electrically insulate the coil from the screws, and holes are rendered leak tight using EDPM⁵ O-rings. Two long O-rings pressed in the inner and outer sides of the cap ensure that the ensemble is leak-tight⁶ up to 4 bars overpressure.

Electric current is injected and collected via two copper plates separated by a thin electrical insulation, minimizing stray magnetic fields (see figure 1). Current is collected from the inner side via a copper screw going through the coil itself. This configuration, made possible by our machinable coil concept, further optimizes the use of space and minimizes stray fields since it does not require an electrical wire running from the inner part of the coil⁷.

The resulting system shown in figure 2 is highly compact. The cap is used to suspend the ensemble such that all the available space of the reentrant viewport is occupied by current carrying copper, maintained as close as possible to the vacuum chamber surface but mechanically disconnected from it.

²Sicomini SR1710/SD7820

³Sigma Aldrich 10 μ m powder, $\geq 98\%$ purity

⁴Polyether ether ketone

⁵EDPM 70, Shore A, 1.5 mm cord, 6 mm diameter

⁶We use Curil T (Elring) grease for matching the O-rings with the surface.

⁷We use Chemtronics CW7100 grease for contact between the copper bolt and the windings

4 Performance

4.1 Magnetic field distribution

The vertical component of the magnetic field B_z produced by the electromagnet was measured with a uniaxial Hall probe⁸ as a function of position. The results are presented in figure 3. For comparison, we performed numerical simulations using the Radia package [19] considering homogeneous current distributions inside the coil body. These are presented as dashed lines in the figure, showing very good agreement with the measurements.

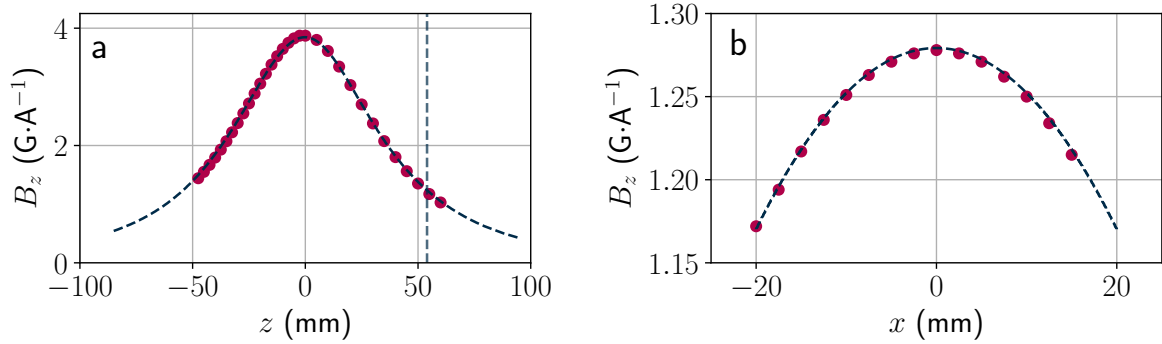


Figure 3: Vertical component of the magnetic field created by one electromagnet **a**: as a function of the position z along the coil axis, and **b**: the position x in the plane of the atoms located 43 mm from the last surface of the coil (dashed vertical line on **a**). The red points are measurements, and the dashed lines represent simulations using the Radia package.

We measured a peak magnetic field at the expected position of the atoms (43 mm below the bottom of the coil) of 1.28 GA^{-1} , implying that a pair of such electromagnet will yield a field of 832.2 G, the position of the broad Feshbach resonance of Lithium [17], at a current of 325 A. The simulation also showed that the current carried in the through hole from the inner to outer winding, which breaks the cylindrical symmetry of the ensemble, results in negligible disturbance in the field distribution.

4.2 Heat management

We tested the thermal performance of the electromagnet by measuring the temperature at different points of the assembly during operation. We first imposed a fixed cooling water flux of $0.23 \text{ l}\cdot\text{s}^{-1}$. The steady state temperature as a function of current is presented in figure 4 at various locations in the system. The overall temperature of the coil body, except for the first inner and outer winding, measured on the bottom side of the coil, remains below 30°C . This confirms our expectations that heat is efficiently removed by water running over the edges of the coil windings. The heating rate of the coil body is $9.4 \text{ K}\cdot\text{kW}^{-1}$.

The increase of the water temperature across the system was very low, and remained lower than at any other point in the electromagnet, confirming that the electromagnet operates in the transfer-limited regime. We observed that temperature is larger at the inner and outer

⁸Lakeshore 425 with HMNA-1904-VR probe

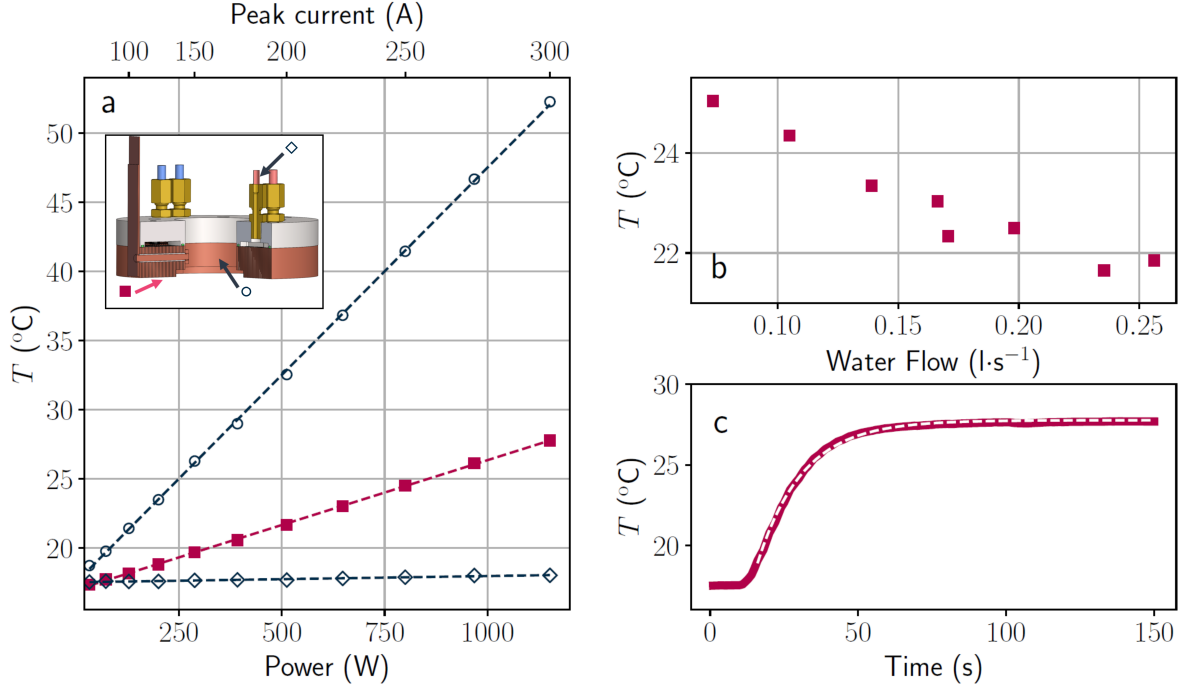


Figure 4: **a:** Steady state temperature of the electromagnet as a function of electrical power dissipated with a total coolant flux of $0.23 \text{ l}\cdot\text{s}^{-1}$, measured at the inner winding (circles), and bottom surface (squares), and temperature of the water exiting the magnet (diamonds). The dashed lines are linear fit to the data, yielding heating rates of 0.45 , 9.4 and $30 \text{ K}\cdot\text{kW}^{-1}$ for the water, coil body and inner winding, respectively. **b:** Temperature of the coil body as a function of the total water flux in the coil, for an average electrical power of 512 W . **c:** Time evolution of the temperature of the coil body following a sudden switch-on of 300 A . The thick red line represents measurements and the dashed line is an exponential fit yielding a timescale of 15.26 s .

windings than in the bulk of the ensemble, because these windings are not in direct contact with water, as can be observed in figure 1. This results from the design choice to privilege the number of windings over the thermal homogeneity⁹. Operating the electromagnet in realistic experimental conditions, with 350 A current and a duty cycle of 30% , we observed that the highest temperature was reached in the inner winding, with a steady-state value of 34°C , compatible with routine operations in the lab.

We then measured the temperature variations with coolant flux. Thanks to the wide section of the coolant circuit, the water flux was only limited by the diameter of the inlet pipes, allowing for total fluxes up to $0.261 \cdot \text{s}^{-1}$ for a moderate water pressure drop of 3.5 bars across the electromagnet. The heating of the coil body is reduced upon increasing the water flux, which is expected due to the dependence of the heat transfer coefficient on velocity in the turbulent regime.

⁹Using the same machining capabilities, our concept allows for the use of a variable pitch spiral ensuring direct water cooling of each winding. In the present case, this would have reduced the number of windings by ~ 4

Last, we measured the dynamics of the thermalization of the coils, monitoring the temperature after switching on the electrical current to 300 A, with a water flux of $0.23 \text{ l}\cdot\text{s}^{-1}$. The result is shown in figure 4c. The evolution is well fitted by a single exponential, which timescale τ allows for an estimate of the average copper-water heat transfer coefficient h : energy balance considerations, supposing a homogeneous temperature within the coil, yields $\tau \sim wC_{\text{Cu}}/h = 15.3 \text{ s}$, with C_{Cu} the specific heat of copper, from which we obtain $h \sim 5 \cdot 10^3 \text{ W}\cdot\text{m}^{-2}\text{K}^{-1}$, in agreement with our initial expectations.

5 Conclusions

We have presented a compact and flexible electromagnet concept adapted to quantum gas experiments requiring both large homogeneous magnetic fields and minimal space occupation. The overall costs are minimal, limited to that of the raw copper, inexpensive epoxy glue, and a home made custom plastic mold for the gluing operation. Cutting the spiral required ~ 40 hours on the wire erosion machine of our institute’s mechanical workshop, running fully automatically.

Our experimental system is constrained by the need for high numerical aperture together with the accommodation of a large, in-vacuum experimental platform, leaving only limited space for the main electromagnets. Thanks to the compactness of the main electromagnets, the reentrant viewports of our experimental setup can also accommodate 4 pairs of compensation coils in the cloverleaf configuration [20], allowing for moving the saddle point of the field in the plane of the coil, a feature which revealed crucial in transport measurements with lithium quantum gases [21].

Acknowledgements

We acknowledge the technical assistance of Claude Amendola, Olivier Haldimann, Gilles Grandjean, Philippe Zuercher and Damien Fasel.

Funding information We acknowledge funding from the ERC project DECCA (Project No. 714309), the Sandoz Family Foundation-Monique de Meuron program for Academic Promotion and EPFL.

References

- [1] H. J. Metcalf and P. van der Straten, *Laser cooling and trapping of atoms*, Journal of the Optical Society of America B Optical Physics **20**, 887 (2003), doi:10.1364/JOSAB.20.000887.
- [2] C. Chin, R. Grimm, P. Julienne and E. Tiesinga, *Feshbach resonances in ultracold gases*, Rev. Mod. Phys. **82**, 1225 (2010), doi:10.1103/RevModPhys.82.1225.
- [3] S. C. Bell, M. Junker, M. Jasperse, L. D. Turner, Y.-J. Lin, I. B. Spielman and R. E. Scholten, *A slow atom source using a collimated effusive oven and a single-layer vari-*

- able pitch coil zeeman slower*, Review of Scientific Instruments **81**(1), 013105 (2010), doi:<http://dx.doi.org/10.1063/1.3276712>.
- [4] P. Cheiney, O. Carraz, D. Bartoszek-Bober, S. Faure, F. Vermersch, C. M. Fabre, G. L. Gattobigio, T. Lahaye, D. Guéry-Odelin and R. Mathevet, *A zeeman slower design with permanent magnets in a halbach configuration*, Review of Scientific Instruments **82**(6), 063115 (2011), doi:[10.1063/1.3600897](https://doi.org/10.1063/1.3600897).
 - [5] F. Bitter, *The design of powerful electromagnets part ii. the magnetizing coil*, Review of Scientific Instruments **7**(12), 482 (1936), doi:[10.1063/1.1752068](https://doi.org/10.1063/1.1752068).
 - [6] F. Bitter, *Water cooled magnets*, Review of Scientific Instruments **33**(3), 342 (1962), doi:[10.1063/1.1717838](https://doi.org/10.1063/1.1717838).
 - [7] D. O. Sabulsky, C. V. Parker, N. D. Gemelke and C. Chin, *Efficient continuous-duty bitter-type electromagnets for cold atom experiments*, Review of Scientific Instruments **84**(10), 104706 (2013), doi:[10.1063/1.4826498](https://doi.org/10.1063/1.4826498).
 - [8] L. Ricci, L. M. Martini, M. Franchi and A. Bertoldi, *A current-carrying coil design with improved liquid cooling arrangement*, Review of Scientific Instruments **84**(6), 065115 (2013), doi:<http://dx.doi.org/10.1063/1.4811666>.
 - [9] R. Wang, M. Liu, F. Minardi and M. Kasevich, *Reaching ^7Li quantum degeneracy with a minitrap*, Phys. Rev. A **75**, 013610 (2007), doi:[10.1103/PhysRevA.75.013610](https://doi.org/10.1103/PhysRevA.75.013610).
 - [10] R. Saint, W. Evans, Y. Zhou, T. Barrett, T. M. Fromhold, E. Saleh, I. Maskery, C. Tuck, R. Wildman, F. Oručević and P. Krüger, *3d-printed components for quantum devices*, Scientific Reports **8**(1), 8368 (2018), doi:[10.1038/s41598-018-26455-9](https://doi.org/10.1038/s41598-018-26455-9).
 - [11] Y. Zhou, N. Welch, R. Crawford, F. Oručević, F. Wang, P. Krüger, R. Wildman, C. Tuck and T. M. Fromhold, *Design of Magneto-Optical Traps for Additive Manufacture by 3D Printing*, ArXiv e-prints (2017), 1704.00430.
 - [12] R. Folman, P. Krüger, J. Schmiedmayer, J. Denschlag and C. Henkel, *Microscopic Atomic Optics: From Wires to an Atomic Chip*, Advances in Atomic and Molecular Physics **48**, 263 (2002), 0805.2613.
 - [13] J. Reichel, *Microchip traps and Bose-Einstein condensation*, Applied Physics B: Lasers and Optics **74**, 469 (2002), doi:[10.1007/s003400200861](https://doi.org/10.1007/s003400200861).
 - [14] H. J. Lewandowski, D. M. Harber, D. L. Whitaker and E. A. Cornell, *Simplified system for creating a bose-einstein condensate*, Journal of Low Temperature Physics **132**(5), 309 (2003), doi:[10.1023/A:1024800600621](https://doi.org/10.1023/A:1024800600621).
 - [15] Y. Long, F. Xiong, V. Gaire, C. Caligan and C. V. Parker, *All-optical production of ^6Li molecular bose-einstein condensates in excited hyperfine levels*, Phys. Rev. A **98**, 043626 (2018), doi:[10.1103/PhysRevA.98.043626](https://doi.org/10.1103/PhysRevA.98.043626).
 - [16] B. Gänger, J. Phieler, B. Nagler and A. Widera, *A versatile apparatus for fermionic lithium quantum gases based on an interference-filter laser system*, Review of Scientific Instruments **89**(9), 093105 (2018), doi:[10.1063/1.5045827](https://doi.org/10.1063/1.5045827).

- [17] G. Zürn, T. Lompe, A. N. Wenz, S. Jochim, P. S. Julienne and J. M. Hutson, *Precise characterization of Li feshbach resonances using trap-sideband-resolved rf spectroscopy of weakly bound molecules*, Phys. Rev. Lett. **110**, 135301 (2013), doi:10.1103/PhysRevLett.110.135301.
- [18] J. Taine, F. Enguehard and E. Lacona, *Transferts thermiques: Introduction aux transferts d'énergie*, Dunod, ISBN 9782100714582 (2014).
- [19] O. Chubar, P. Elleaume and J. Chavanne, *A three-dimensional magnetostatics computer code for insertion devices*, Journal of Synchrotron Radiation **5**(3), 481 (1998), doi:10.1107/S0909049597013502.
- [20] M.-O. Mewes, M. R. Andrews, N. J. van Druten, D. M. Kurn, D. S. Durfee and W. Ketterle, *Bose-einstein condensation in a tightly confining dc magnetic trap*, Phys. Rev. Lett. **77**(3), 416 (1996), doi:10.1103/PhysRevLett.77.416.
- [21] S. Krinner, T. Esslinger and J.-P. Brantut, *Two-terminal transport measurements with cold atoms*, Journal of Physics: Condensed Matter **29**(34), 343003 (2017).